# DAMPING OF SLOSHING DUE TO TANK ROOF IMPACT

Olav F. Rognebakke and Odd M. Faltinsen
Department of Marine Hydrodynamics
Norwegian University of Science and Technology
N-7491 Trondheim, Norway

A partially filled smooth tank will experience violent fluid motion when forced to oscillate with a period close to the highest natural period of the fluid motion. When the free surface hits the tank roof, a water impact similar to slamming occurs, and energy is dissipated. A statistical treatment of sloshing demands time efficient calculations. Thus, the analytic approach proposed by Faltinsen et al. [1] is well suited for the task. However, the analytical model does not account for impact of water on the roof. By estimating the kinetic and potential energy loss in the jet generated during the impact and relating this to the total energy in the fluid, an equivalent damping term can be introduced in the analytical model. A Wagner's method [2] is applied. When the impact angle between the rising free surface and a chamfered tank roof is large, results from a similarity solution are utilized to correct the estimated energy loss. Numerical simulations for the free surface elevations for a heavy impact case are compared with experimental results. Numerical force calculations and experimental data for different fluids are presented for an LNG tank model.

Consider a rectangular smooth and rigid tank forced to oscillate harmonically in surge. The fluid is incompressible and the flow is two-dimensional and irrotational. The height and the breadth of the tank are $H$ and $l$. The coordinate system $(x, z)$ is fixed relative to the tank with origin in the mean free surface and in the center of the tank (See Fig. 1.). Violent fluid motion will occur due to resonant motions and small damping. For non-impacting fluid flow, the damping is very small and mainly due to viscosity in the boundary layers [3]. Nonlinearities are significant and cause finite amplitudes at resonance.

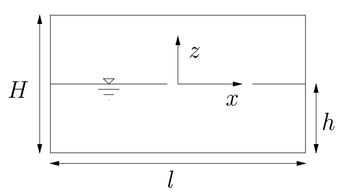


Figure 1: Coordinate system and tank dimensions.

When the fluid motion does not impact the tank roof, [1] is applied. This is based on a Bateman-Luke variational principle and use of the pressure in the Lagrangian of the Hamilton principle. This results in a system of nonlinear ordinary differential equations in time. The unknowns are generalized coordinates $\beta_i$ of the free surface elevation. The procedure applies to any tank shape as long as the tank walls are vertical near the mean free surface. The equation system for the rectangular tank excited in surge, heave and pitch follows. The free surface elevation $\zeta$ is written as

$$\zeta = \sum_{i=1}^{N} \beta_i(t) \cos\left(\frac{\pi i(x + 0.5l)}{l}\right) \tag{1}$$

The forced oscillation amplitude is assumed small and of $O(\epsilon)$. Further $\beta_i = O(\epsilon^{\frac{i}{3}})$ , $i = 1, 3$. Higher order terms than $\epsilon$ are neglected in the nonlinear equations. The following system of nonlinear ordinary differential equations for the generalized coordinates describing the free surface are derived for forced motions

$$\begin{gathered}
(\ddot{\beta}_1 + \sigma_1^2\beta_1) + d_1(\ddot{\beta}_1\beta_2 + \dot{\beta}_1\dot{\beta}_2) + d_2(\ddot{\beta}_1\beta_1^2 + \dot{\beta}_1^2\beta_1) + d_3\ddot{\beta}_2\beta_1 + P_1(\dot{v}_{0x} - S_1\dot{\omega} - g\psi) + Q_1\dot{v}_{0z}\beta_1 = 0,\\
(\ddot{\beta}_2 + \sigma_2^2\beta_2) + d_4\ddot{\beta}_1\beta_1 + d_5\dot{\beta}_1^2 + Q_2\dot{v}_{0z}\beta_2 = 0,\\
(\ddot{\beta}_3 + \sigma_3^2\beta_3) + d_6\ddot{\beta}_1\beta_2 + d_7\ddot{\beta}_1\beta_1^2 + d_8\ddot{\beta}_2\beta_1 + d_9\dot{\beta}_1\dot{\beta}_2 + d_{10}\dot{\beta}_1^2\beta_1 + P_3(\dot{v}_{0x} - S_3\dot{\omega} - g\psi) + Q_3\dot{v}_{0z}\beta_3 = 0,\\
\ddot{\beta}_i + \sigma_i^2\beta_i + P_i(\dot{v}_{0x} - S_i\dot{\omega} - g\psi) + Q_i\dot{v}_{0z}\beta_i = 0, \quad i \geq 4.
\end{gathered} \tag{2}$$

Here $v_{0x}$ and $v_{0z}$ are projections of translational velocity onto axes of $Oxz$ and $\omega(t)$ is the value of angular velocity of coordinate system $Oxyz$ with respect to an earth fixed coordinate system. The calculation formulas for the coefficients $\sigma_i$, $P_i$, $S_i$, $Q_i$, $i \geq 1$ and $d_j$, $j = 1, \ldots, 10$ are given in [1]. The equation system is solved numerically by a fourth order Runge-Kutta method.

When the water impacts on the tank roof, fluid damping is believed to occur. The hypothesis is that the kinetic and potential energy in the jet flow caused by the impact is dissipated. Fig. 2 shows the evolution of an impact in the upper left corner of an LNG ship tank. The formation and overturning of the jet are evident. The linear damping terms $2\xi\sigma_i\dot{\beta}_i$ are included in each of eq. 2. The damping is found as an equivalent damping so that the energy $\Delta E$ removed from the system during one full cycle is equal to the kinetic and potential energy lost in the impact, i.e. $\xi = \frac{1}{4\pi}\frac{\Delta E}{E}$. $E$ is the total energy in the system, which is found from $\dot{E} = F_x v_{0x}$ for forced surge motion. An iterative procedure is followed. A simulation over one

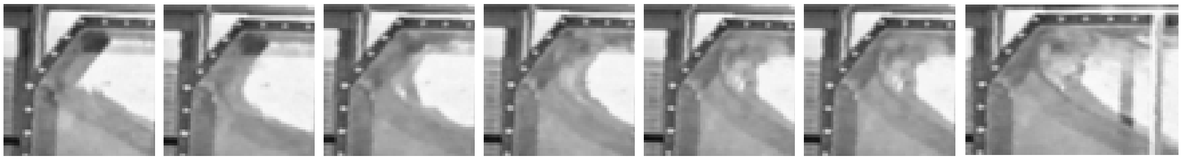

Figure 2: Snapshots of upper left corner of LNG tank during impact

period is started with no damping. A first estimate of $\xi$ is found. The simulation is repeated, which results in a new $\Delta E$ and thereafter a new $\xi$. This is done for iteration $i > 1$ as $0.5\frac{\Delta E_i + \Delta E_{i-1}}{E} = 4\pi\xi$. Typically, 5 iterations are sufficient for convergence.

The impact model is based on a generalized Wagner's approach [2]. The tank is assumed rigid so possible hydroelastic effects are ignored. The inflow velocity $V(t)$ and the slope of the impacting surface can be found directly from Eq. 1. The impact velocity is approximated by a linear function $V(t) = V_0 + V_1 t$. $t = 0$ is the time of impact. The impacting surface is approximated by a parabola with radius of curvature $R$. The wetted length $c(t)$ follows from Wagner's integral equation. This solution can be corrected by accounting for the tank walls and bottom. Details can be found in [4]. However, this effect is not important and thus is not included here. The Wagner's analysis assumes a small angle between undisturbed free surface and tank roof. A similarity solution presented by Zhao and Faltinsen [5], valid for large angles, is applied to correct the energy estimates when this is not the case. The energy estimates obtained from Wagner's analysis are multiplied by a reduction factor. Fig. 3 gives the definitions of symbols used in the slamming analysis. $c(t)$ is the horizontal distance from $x = 0$ to the spray root, $\delta$ is the thickness of the jet, $u_c$ is the velocity of the control surface following the spray root and $u_a$ is the fluid velocity in the jet direction at the spray root. Fig. 4 introduces symbols applied in the similarity solution. $s_j$ is the length of the jet, $\beta$ is the deadrise angle of the wedge, $\beta_0$ is the angle of the triangular jet and $\zeta_L$ and $\zeta_B$ are the vertical distances to the jet root and tip of the jet, respectively.

The similarity solution is derived for a constant impact velocity. However, the reduction factor found for the energy loss for a constant speed is also applied for the linearly decreasing impact velocity.

The kinetic energy flux into the jet is calculated for both the similarity solution and Wagner's approach for a wedge and constant impact speed. The kinetic and potential energy flux through the jet can generally be found as

$$\frac{\mathrm{d}E_{kin}}{\mathrm{d}t} = \frac{\rho}{2} u_a^2 \delta u_f \quad , \quad \frac{\mathrm{d}E_{pot}}{\mathrm{d}t} = \rho g (H - h) M_{\text{flux}} \tag{3}$$

when a constant velocity across the jet is assumed, and the potential energy loss is estimated as the potential energy the mass of the water in the jet has relative to the level of the mean free surface. $u_f$ is the relative velocity between the fluid velocity and the control surface velocity, $u_f = u_a - u_c$. $M_{\text{flux}} = \delta u_f$ is the flux of mass into the jet. Wagner's solution gives [5]

$$u_a = 2\frac{\mathrm{d}c}{\mathrm{d}t} \quad , \quad u_c = \frac{\mathrm{d}c}{\mathrm{d}t} \quad , \quad c = \frac{\pi V t}{2\tan(\beta)} \quad , \quad \delta = \frac{\pi V^2 2c}{16(\frac{\mathrm{d}c}{\mathrm{d}t})^2} = \frac{\tan(\beta) V t}{4} \tag{4}$$

The kinetic energy flux and mass flux is then

$$\left.\frac{\mathrm{d}E_{kin}}{\mathrm{d}t}\right|_W = \frac{\rho V^4 \pi^3 t}{16\tan^2(\beta)} \quad , \quad M_W = \frac{\mathrm{d}c}{\mathrm{d}t}\delta = \frac{\pi V^2}{8} t \tag{5}$$

The jet in the similarity solution is assumed to be triangular, giving

$$\frac{s_j}{Vt} = \frac{\xi_B - \xi_L}{Vt\sin(B)} \quad , \quad \frac{\delta}{Vt} = \frac{s_j}{Vt}\tan(\beta_0) \tag{6}$$

The mass flux into the jet is then equal to

$$M_S = \frac{\mathrm{d}}{\mathrm{d}t}\left[\frac{1}{2}s_j\delta\right] = \frac{\mathrm{d}}{\mathrm{d}t}\left[\frac{1}{2}(\frac{\zeta_B - \zeta_L}{\sin(\beta)})^2 \tan(\beta_0)\right] = \left[\frac{\zeta_B - \zeta_L}{Vt\sin(\beta)}\right]^2 \tan(\beta_0) V^2 t \tag{7}$$

A constant flux velocity in the similarity solution is found as $u_f = \frac{M_S}{\delta}$. By observing that the $z$ component of $u_c$ must be equal to $\mathrm{d}\zeta_L/\mathrm{d}t$ plus the constant downward velocity $V$, $u_c$ can be estimated as

$$u_c = \frac{\mathrm{d}\zeta_L/\mathrm{d}t}{\sin(\beta)} + \frac{V}{\sin(\beta)} \tag{8}$$

Again, substituting in Eq. 3, the kinetic energy flux for the similarity solution is

$$\left.\frac{\mathrm{d}E_{kin}}{\mathrm{d}t}\right|_S = \frac{\rho V^4 t \tan(\beta_0)}{2\sin^4(\beta)}\left[\left(\frac{\mathrm{d}\zeta_L/\mathrm{d}t}{V}\right)+1+\frac{\zeta_B-\zeta_L}{Vt}\right]^2\left[\frac{\zeta_B-\zeta_L}{Vt}\right]^2 \tag{9}$$

Figs. 5 and 6 show the difference in kinetic energy and mass flux for Wagner's approach and the similarity solution. The numerical results are based on numbers presented in [5]. When $\beta \to 0$, the results by the similarity solution and Wagner agree. It is planned to derive a solution for finite deadrise angle that matches the local jet flow and the global solution. This will give more rational estimates of energy loss during an impact with changing impact velocity. Using analytically based computations are advantageous relative to a direct numerical approach due to the extremely fine discretization needed both in time and space in order to capture the details of a jet flow.

The free surface elevation is compared with experimental results for a heavy impact case in Fig. 7. The tank is rectangular with $l = 1.73$m, a filling height $h = 0.5$m and a total height of $H = 1.02$m. The tank roof is horizontal. The period and amplitude of the sway excitation are $T = 1.71$s and $\epsilon_0 = 0.05$m, respectively. The figure suggests that a satisfactory estimate of the impact velocity $\mathrm{d}\zeta/\mathrm{d}t$ can be calculated. This value is important in the prediction of slamming loads.

Fig. 8 shows the dimensions of the prismatic LNG tank model for which computational and experimental results of horizontal forces are presented in Fig. 9. The experimental results are found in [6]. A small ever-present non-impact damping was introduced and time series of 400s simulated in order to reach a steady state motion. The chamfer angle is 45 degrees. This gives a reduction factor for the kinetic energy loss of 0.27 and a factor of 0.22 for the potential energy loss. Wagner's approach heavily over-predicts the energy loss for large angles. A good agreement is seen for results away from resonance. At resonance the current approach predicts too large forces. However, if no impact damping was introduced, the maximum force was far larger, about 1.4 times the one presented. Sources of error are discussed below.

The energy loss through the jet and evolution of the wetted length $c(t)$ are shown in Fig. 10. In this special case, approximately 1/5 of the total energy in the fluid is lost during the two impacts of one cycle. The kinetic and potential energy loss are of similar magnitude. The main part of the energy loss happens during the initial phase of the impact. Hence, the errors due to an assumption of a linearly decreasing impact velocity and constant free surface curvature should not be large. At $t = 35.425$ the impact moves past the chamfered part of the roof.

There are several uncertainties and sources of error in the presented methodics, of which some have been discussed already. The accuracy of the nonlinear flow model is of great importance. Missing nonlinear effects can for an excitation close to resonance result in a misprediction of the maximum free surface elevation, leading to a relatively larger error in the estimation of the damping level. This will be investigated by using a fifth order theory, which is a further development of [1]. Local downward vertical accelerations above 1g are calculated for some impact cases. According to Penney and Price [7] this is a criterion for breaking of a standing wave. The only back-coupling from the impact to the analytic model is through damping. When the duration and spatial extent of the impact are large, this simplification may no longer suffice.

Force calculation neglects the horizontal force directly caused by the impact. It means that the horizontal force is calculated like in [1]. The additional force has a magnitude of approx. 10% of the total force for a heavy impact in the LNG tank. The impulse is close to zero.

Further work will also focus on the continued development of a nonlinear boundary element method designed for calculating the impact jet flow. This approach will serve to validate the current methodics, as well as provide an alternative damping estimate for heavy impact situations. The wish to still use the nonlinear analytical method for the non-impact flow is motivated by the dramatic difference in simulation time.

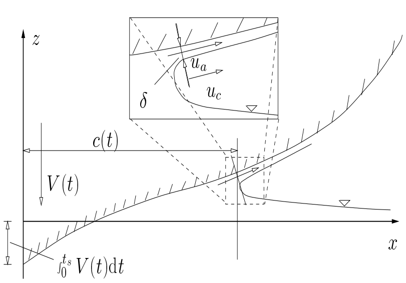


Figure 3: Definitions for the slamming analysis

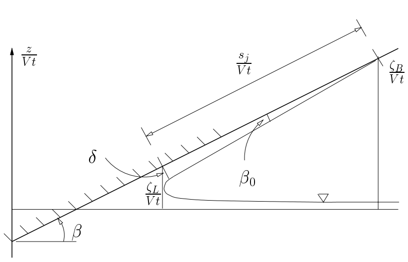


Figure 4: Definitions used in the similarity solution

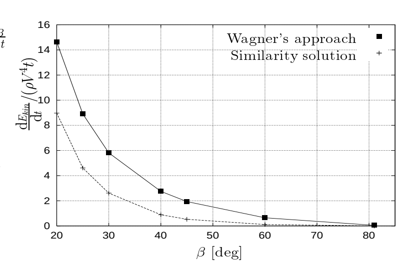


Figure 5: Kinetic energy flux

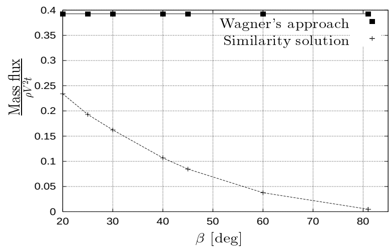


Figure 6: Mass flux

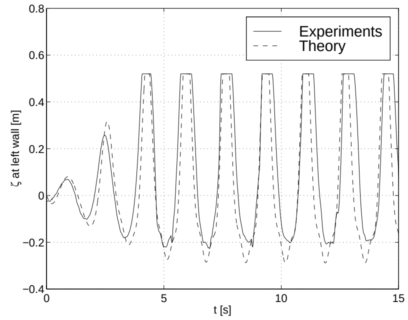


Figure 7: Free surface elevation for a case of heavy roof impact

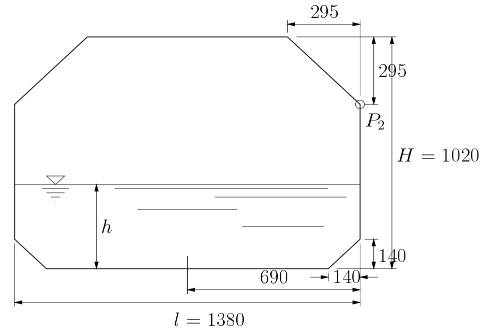


Figure 8: Prismatic LNG tank model. All numbers in [mm]

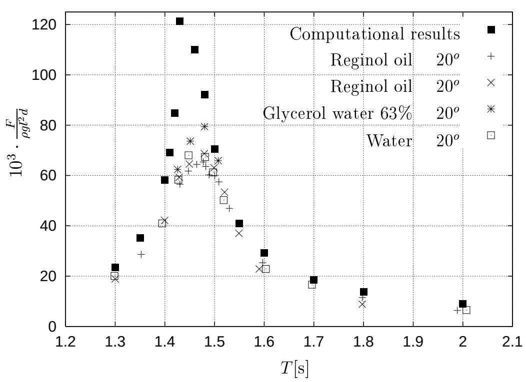


Figure 9: LNG tank $\frac{h}{l} = 0.4$, $\frac{\epsilon_0}{l} = 0.01$. Computational results and experimental data for various fluids

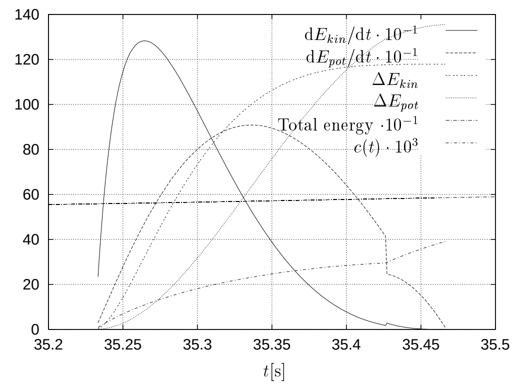


Figure 10: LNG tank $\frac{h}{l} = 0.4$, $\frac{\epsilon_0}{l} = 0.01$ and $T = 1.43$s. Change of energy during an impact

## Acknowledgements

This work is part of a Ph. D. thesis sponsored by the Research Council of Norway.

## References

[1] Faltinsen, O. M., Rognebakke, O. F., Lukovsky, I. A., Timokha, A. N. Multidimensional modal analysis of nonlinear sloshing in a rectangular tank with finite water depth. Accepted for publication in *J. Fluid Mech.*.

[2] Wagner, H. (1932) Über Stoss- und Gleitvorgänge and der Oberflache von Flussigkeiten. Zeitschr. F. Angew. *Math. und Mech.* **12**, 193-235

[3] Keulegan, G. H. (1958) Energy dissipation in standing waves in rectangular basins. *J. Fluid Mech.* **6**, 33-50

[4] Faltinsen, O. M., Rognebakke, O. F. (1999) Sloshing and slamming in tanks. *HYDRONAV'99-MANOEUVERING'99* Gdansk-Ostrada, Poland

[5] Zhao, R., Faltinsen, O. M. (1993) Water entry of a two-dimensional bodies. *J. Fluid Mech.* **246**, 593-612

[6] Faltinsen, O. M., Olsen, H. A., Abramson, H. N., Bass, R. L. (1974) Liquid slosh in LNG carriers. Det Norske Veritas, Publication No. **85**

[7] Penney, W. G., Price, A. T. (1952) Finite Periodic Stationary Gravity Waves in a Perfect Liquid. *Phil. Trans. Royal Soc.* (London) **A 244**, 254-284